



An approach to understand the uranium's concentration variance on the eastern and western sides of the Nile Valley phosphorites, Egypt

Sameh H. Negm¹

Received: 29 November 2023 / Accepted: 20 February 2024 / Published online: 20 March 2024
© The Author(s) 2024

Abstract

The Nile Valley is a main area for Egyptian phosphorites. The studied samples from the eastern and western sides of the Nile Valley showed similarities in their characteristics, suggesting one depositional basin, but they varied in their uranium content, with averages recorded at 91.7 and 44.83 ppm on the eastern and western sides, respectively. The evidence pointed out that initially the uranium was formed by adsorption onto the iron oxides and organic matter surfaces, then it was partially removed under the effect of groundwater, and the removal was deeper in the western phosphorites than the eastern ones.

Keywords Phosphorites · Egypt · Nile Valley · Uranium

Introduction

Phosphorite deposits are one of the most important economic deposits, as they are the raw materials for many important industries. Phosphorites are well recognized in several countries around the world [1]. Middle East-North Africa (MENA) region, Morocco, Tunisia, Egypt, Jordan, and Syria are major countries with huge phosphorite deposits that are exploited for domestic purposes in addition to being exported as raw materials [2]. Phosphorites are mainly considered for the manufacturing of phosphoric acid and agricultural fertilizers, they are also regarded as non-conventional resources for some economic and strategic elements such as uranium and rare earth elements (REEs) [3].

There are two main types of phosphate rock deposits: sedimentary phosphate and igneous phosphate. Overall, sedimentary phosphate deposits have been exploited to produce more than 80 percent of the world's total production of phosphate rock. Igneous phosphate deposits are often associated with carbonatites and/or alkalic (silica-deficient) intrusions. Igneous phosphate rock concentrates are produced from deposits that are mainly exploited in Russia, the

Republic of South Africa, Brazil, Finland, and Zimbabwe. Igneous phosphate ores are often low in grade (less than 5 percent P_2O_5) [4, 5].

The Egyptian phosphorites belong to the phosphorite belt, which extends along North Africa from the west to the east. The Egyptian phosphorites are composed of three belts. The northern belt, which extends from Sinai to Bahariya Oasis in thin layers and is intercalated by carbonate and sand facies, has no economic potential. The central belt, which is considered almost economic, occupies the subsequent localities: the land stretch along the Red Sea from Safaga to Quseir. The Nile Valley, from Idfu to Qena, and the Western Desert on Abu Tartur Plateau, while the southern belt has been extended through Aswan and is characterized by the association of iron ore accumulations among shallow water sediments. Also, this belt didn't have economic importance [6]. Tens of studies dealt with the Egyptian phosphorites and investigated several issues, such as the depositional conditions, mineralogical and chemical specifications, the geochronological aspect, and more [7–13]

The Nile Valley phosphorites are mainly composed of phosphate and carbonate fractions, while the detrital components represent minor components. The uranium and rare earth elements were found to be related to the phosphate and carbonate components [10, 11, 14, 15]. The trace elements of the Egyptian phosphorites were categorized into four types based on their sources as: (1) trace elements associated with the detrital minerals; (2) trace elements introduced by

✉ Sameh H. Negm
samehnegm.nma@gmail.com

¹ Nuclear Materials Authority, El Maadi, P.O. Box 530, Cairo, Egypt

weathering; (3) trace elements incorporated with the organic matter; and (4) trace elements located within the apatite lattice [16, 17].

The geochemical behavior of uranium in the Egyptian phosphorites was a matter of interest. The relation between P and U contents could be taken as an indicator for the uranium concentration and mobility in the phosphate deposits [18, 19], where the uranium distribution is mainly controlled by the variations in the phosphatic components with no or probable faint affecting by the detrital content. Also, the weak correlation between P and U or Ca and U elements points to probable diagenetic processes that resulted in the re-arrangement, migration-in, and/or migration-out of uranium in the phosphorites. In similar terms, the phosphate deposits of East Luxor, Egypt, have signs of the migration of uranium-rich solutions, and this migration was directed from the depositional basin upward. However, post-consolidation enrichment of uranium was insignificant, as no concentration of uranium is recorded now along fractures or weak zones [19].

Several syngenetic and/or diagenetic factors can affect the uranium contents of the phosphate deposits; one of these factors refers to the depositional depth of the marine phosphorites as a possible reason for uranium enrichment, where the deeper deposition might encourage the uranium enrichment into the apatite lattice more than the shallower deposited marine phosphorites, probably due to the larger exposure of apatite to sea water [20]. Also, the organic matter content of the phosphorites is another significant factor, where there is always an appositive relationship between the organic matter and uranium contents [21].

However, one of the most interesting phenomena that appeared in much literature is the clear variance of the uranium concentrations between the East and West sides of the Nile Valley phosphate deposit, despite the same depositional environment, conditions, and age, where the East Nile Valley phosphorites always record higher uranium content than the West one.

The present study aims to investigate the reasons that caused the difference in uranium concentrations in the Nile Valley phosphates. The study area is divided into two main localities on opposite sides of the Nile River, exhibiting dissimilar uranium percentages despite their geological unity.

Geologic background

The studied phosphorites occur in the Upper Cretaceous Duwi Formation [22], which represents the establishment of the first fully marine condition that extended across Egypt during the major transgression in Late Cretaceous time [23].

The areas under investigation are located on both sides of the Nile River, between Idfu and Qena cities (Fig. 1).

The Duwi Formation in the studied localities is mainly composed of phosphate beds intercalated with shale, marl, oyster limestone, and chert bands. It unconformably overlies the fluvial shale sequence of the Middle Campanian Qusier shale and is overlain conformably by the deep marine shales and marls of the Middle Maestrichtian Dakhla shale. Thus, deposition of Duwi Formation represents an initial stage of the late Cretaceous marine transgression in Egypt (Fig. 2).

The Duwi Formation in the Nile Valley region was divided by [25] into three members (from bottom to top):

- Mahamid Member: composed of shale, clay, sandstone, and carbonaceous shale with a few phosphatic intercalations.
- Sibaiya Member: made up of siliceous-carbonate phosphorite beds intercalated with chert bands and lenses changing upwardly to shale, oyster limestone, and marl.
- Adayma Member: Consists of marl, sandstone, some oyster limestone and phosphate beds.

According to [8], the Duwi Formation in the Nile Valley region was subdivided into three members based on its lithology

- The lower member is composed of quartzose sandstone and siliceous shale.
- The middle member is built up of soft, laminated, and organic-rich black shale.
- The upper member is mainly made up of phosphatic sandstone.

Methodology

For this work, twelve representative phosphorite samples were collected from the economic bed (horizon A) of the Duwi Formation, where six samples were collected from each side of the Nile River. The localities of the collected samples are illustrated in Table 1 and Fig. 3.

The petrographic characteristics of the studied phosphorites were investigated under a Nikon polarizing microscope equipped with an automatic camera and a mechanical stage, while the separated minerals were identified using the X-ray diffraction technique (XRD), and an additional investigation was carried out by the scanning electron microscope attached with an energy dispersive X-ray (SEM–EDX).

On the other hand, the chemical composition of the investigated phosphorite samples was identified and

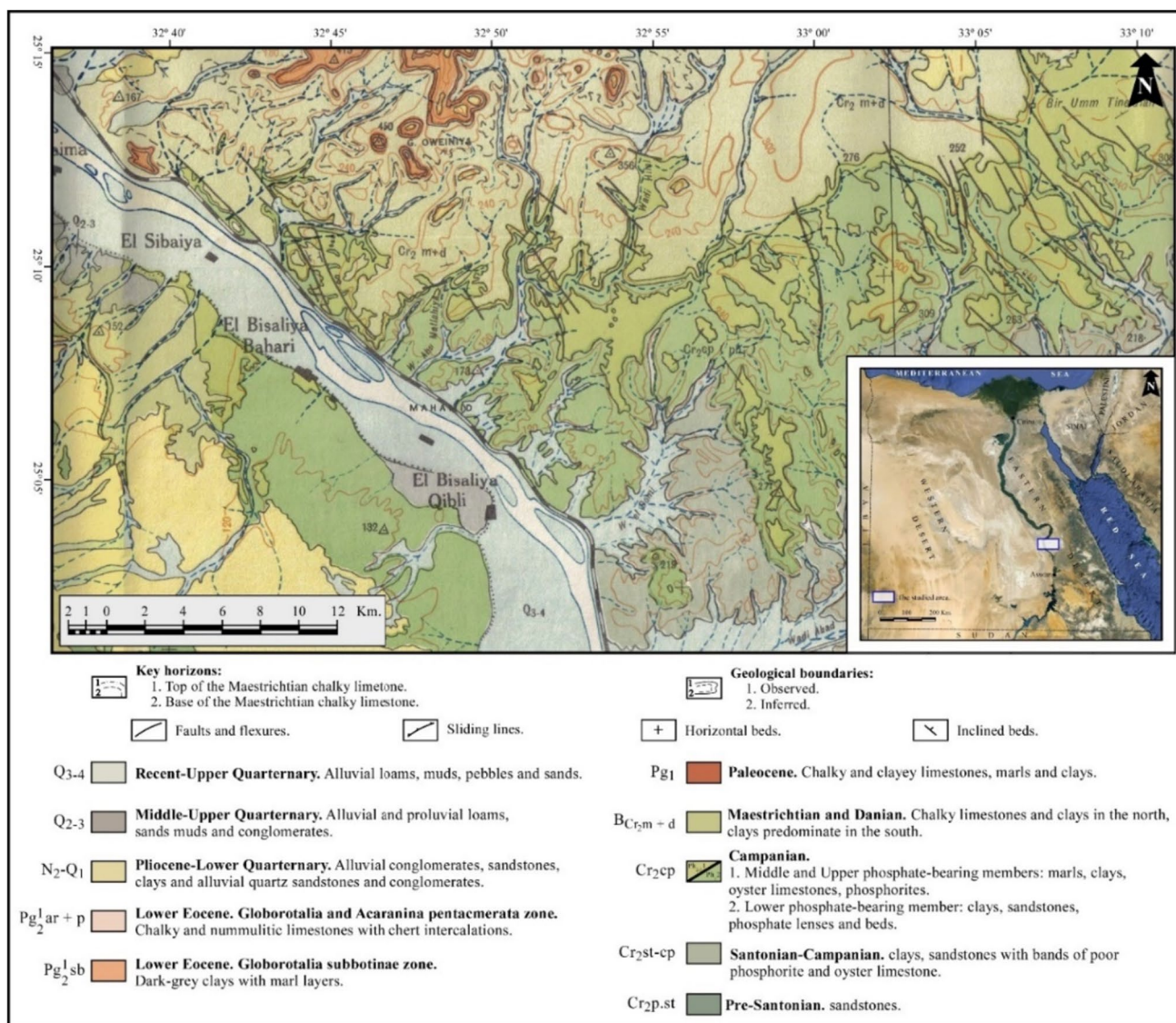


Fig. 1 Geologic map of the studied area, after [24]

quantified either by conventional wet chemical techniques for the major components [26, 27] or using the X-ray fluorescence technique (XRF) for the trace element contents. The uranium, thorium, and radium concentrations were determined by a multi-channel gamma-ray spectrometer. The system consists of a NaI-Tl bicorn scintillation detector connected to an NE-4658 amplifier and a high-voltage power supply with an HV digital display. Additionally, an elemental chemical distribution map for the apatite grains was executed using the microprobe technique (model: JEOL). It is worth mentioning that all the used instruments are installed at the Nuclear Materials Authority in Egypt, except the microprobe instrument, which is installed at

the Naruto University of Education in Naruto, Tokushima, Japan.

The study implemented quality control measures, including the use of Durango apatite as standard reference materials, duplicate analyses, and external proficiency tests. The precision of the geochemical assay procedures was held at $\pm 5\%$.

Statistical analysis

The results are expressed as the average \pm standard error (S.E.) of the sample average, and statistical analysis was

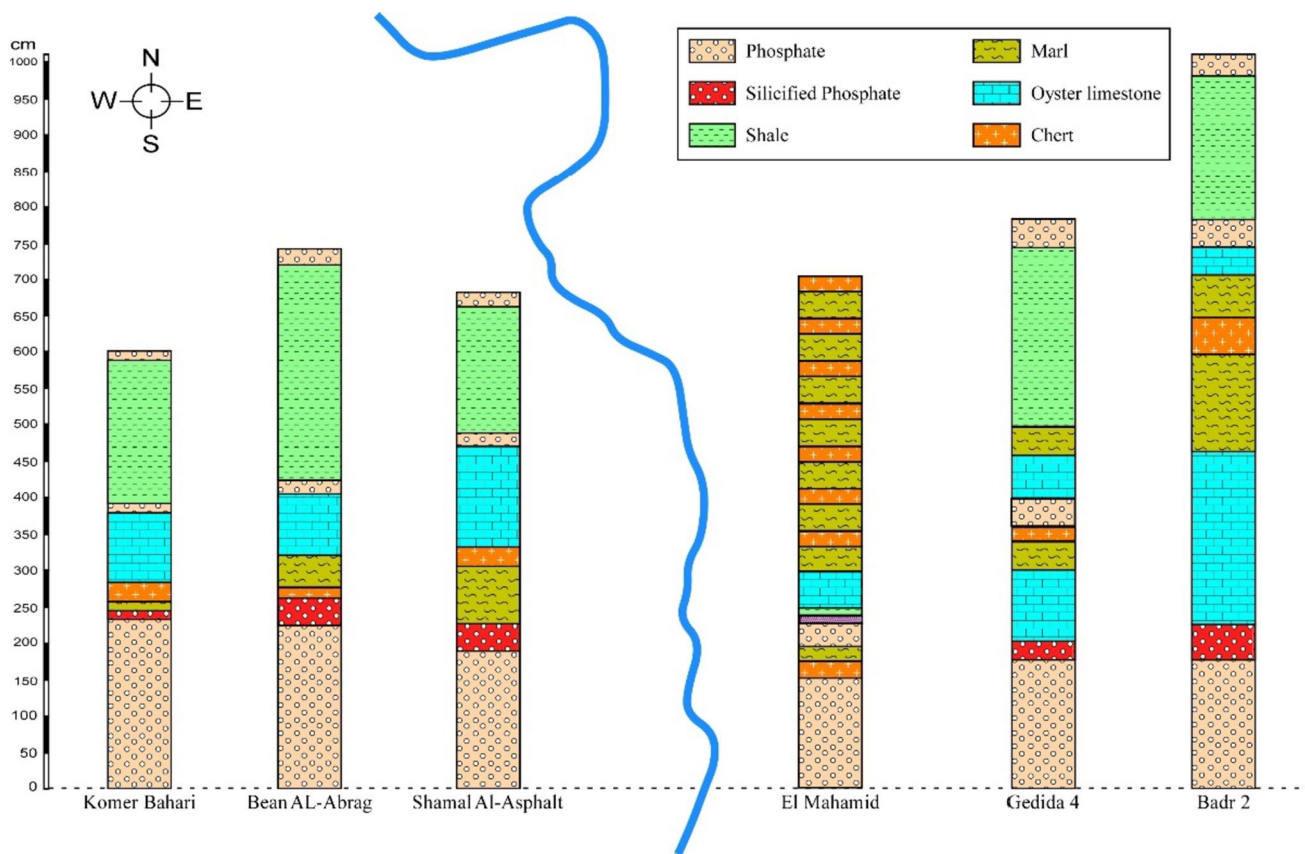


Fig. 2 Lithostratigraphic composite succession of Duwi Formation in the studied localities

Table 1 The collected phosphorites samples information

The Nile Valley side	Localities	Sample number
Eastern side	Badr-2 mine	E-1
		E-2
	Gedida-4 mine	E-3
		E-4
	El Mahamid mine	E-5
		E-6
Western side	Shamal Al-Asphalt mine	W-1
		W-2
	Bean Al-Abrag mine	W-3
		W-4
	Komer Bahari mine	W-5
		W-6

performed using Statistical Package for the Social Science (SPSS) version 20.

Results and discussion

The main mineralogical, geochemical, and radioactivity characteristics of the phosphorites on both sides were a matter of investigation to shed light on the probable reason(s) that caused the uranium concentration variance, despite the same depositional environment and conditions.

Petrography and mineralogy

Petrographically, the Nile Valley phosphorites exhibited different colors, such as pale yellow, yellowish brown, and grayish brown (Fig. 4). This variation in color is likely due to the nature and type of the encountered grains and the cementing material. Also, there is variation in their compaction and hardness, where they vary from dense and very hard to very friable and soft. These properties are controlled mainly by the size and packing of grains, in addition to the texture and composition of the cementing materials.

The phosphatic and non-phosphatic constituents appeared as the main components in the studied phosphorites on

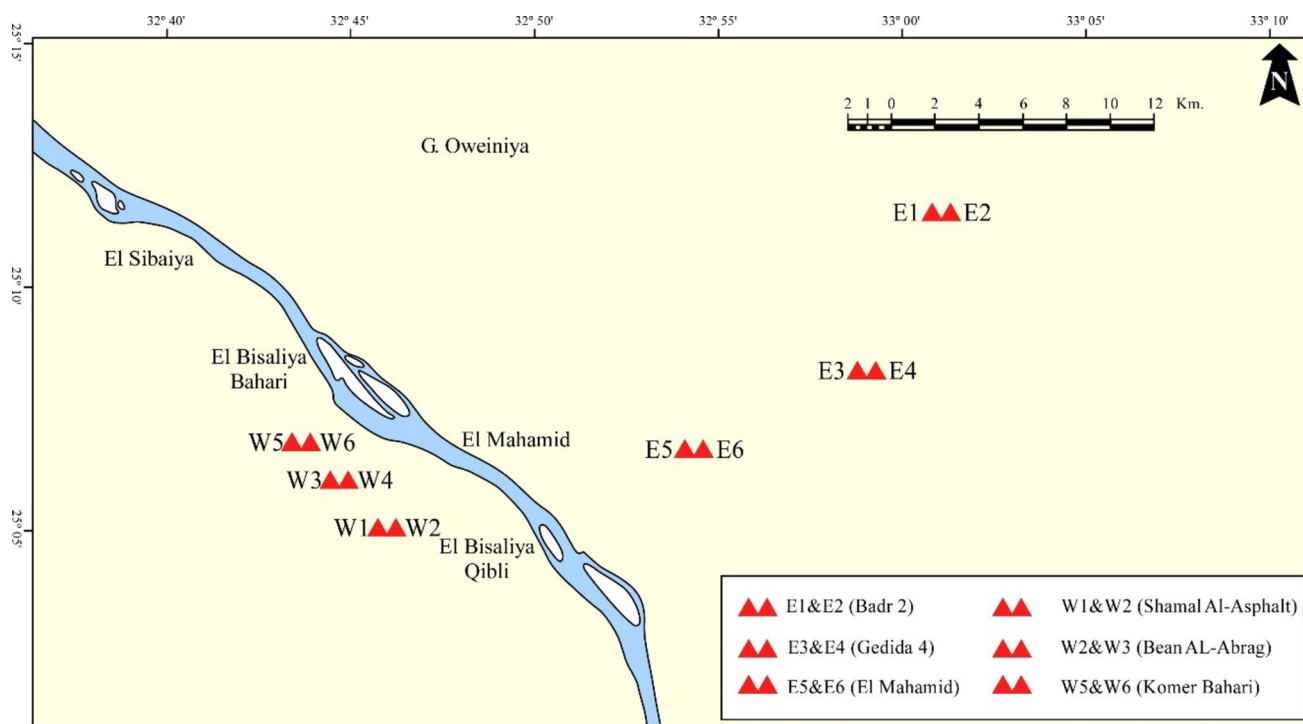
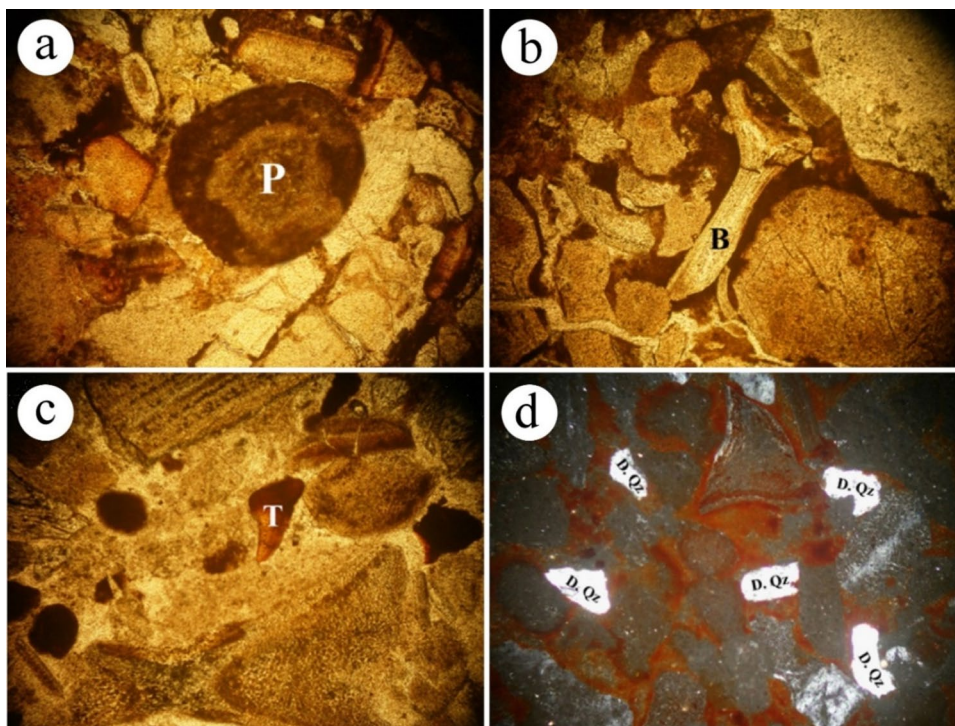


Fig. 3 Site locations map of the studied phosphorites samples

Fig. 4 **a** Photomicrograph showing well-rounded cryptocrystalline homogeneous pellet (P) of collophane (C.N., X=20), **b** Photomicrograph showing large phosphatic bone fragment (B) filled with phosphatic mud (C.N., X=20), **c** Photomicrograph showing coarse teeth fragments (T) embedded in cryptocrystalline collophane (C.N., X=10), and **d** Photomicrograph showing medium detrital quartz grains (D. Qz) (C.N., X=10)



both sides of the Nile Valley phosphorites. In which the phosphatic constituent represents 70% by volume of the

whole studied rock, and they are classified into phosphatic mudclasts (collophane grains) and phosphatic bioclasts

(fish bones and shark's teeth) (Fig. 4). On the other hand, detrital quartz grains, carbonates (as shell fragments), and iron oxides are the main non-phosphatic constituents of the studied phosphorites. Also, the study showed that the West Nile phosphorite is more enriched in silica components, either in the form of detrital quartz grains or as silica cement materials, by which these phosphorites acquired the name silicified-phosphate rock. Occasionally, the pelletal cellophane grains exhibit a dark halo, which might be due to the presence of uranium in the crystal structure of the cellophane grains (Fig. 4a). It is worth mentioning that this observation was recorded in phosphorite samples from the east side, and no observation like that was found in the west side phosphorite.

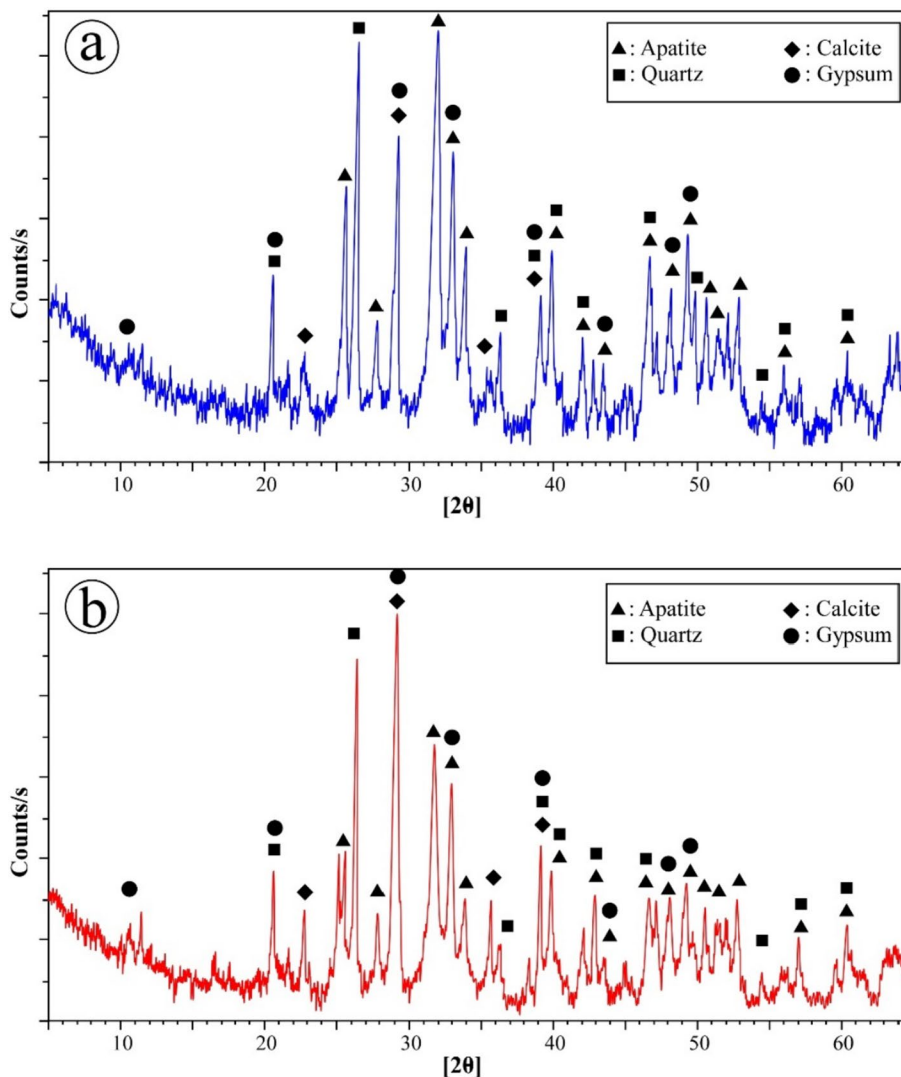
On the other hand, the mineralogical study for whole rock samples using the XRD technique as well as the SEM–EDX investigation for picked grains were matched with the petrographic study, where the main mineralogical components were the phosphatic minerals represented

in the carbonate-fluorapatite (francolite) mineral $\text{Ca}_5[(\text{PO}_4, \text{CO}_3)_3](\text{F}, \text{O})$ as the most abundant apatite type and, to a lesser extent, the carbonate-hydroxyl apatite (dahllite) $\text{Ca}_5[(\text{PO}_4, \text{CO}_3)_3](\text{OH}, \text{O})$ (Figs. 5 and 6). Also, the bone fragment and shark teeth were recorded as phosphatic materials rich in phosphorous and calcium (Fig. 7). The XRD investigation pointed to the relative abundance of the apatite mineral in the east phosphorites compared to the west one, while the quartz mineral showed opposite behavior.

The non-phosphate minerals are found as; quartz grains either enclosed within phosphatic peloids or embedded in the groundmass; the calcite mineral occurs as cement as well as allochemicals; and mainly oyster limestone shells in addition to the gypsum mineral (Fig. 5).

As conducted from the EDX semi-quantitative analyses for the bone fragment and the shark tooth enamel, both components are of apatitic composition, where both Ca and P are the main constituents with minor amounts of

Fig. 5 X-ray diffraction patterns of the studied phosphorite samples (**a** the eastern bank and **b** the western bank)



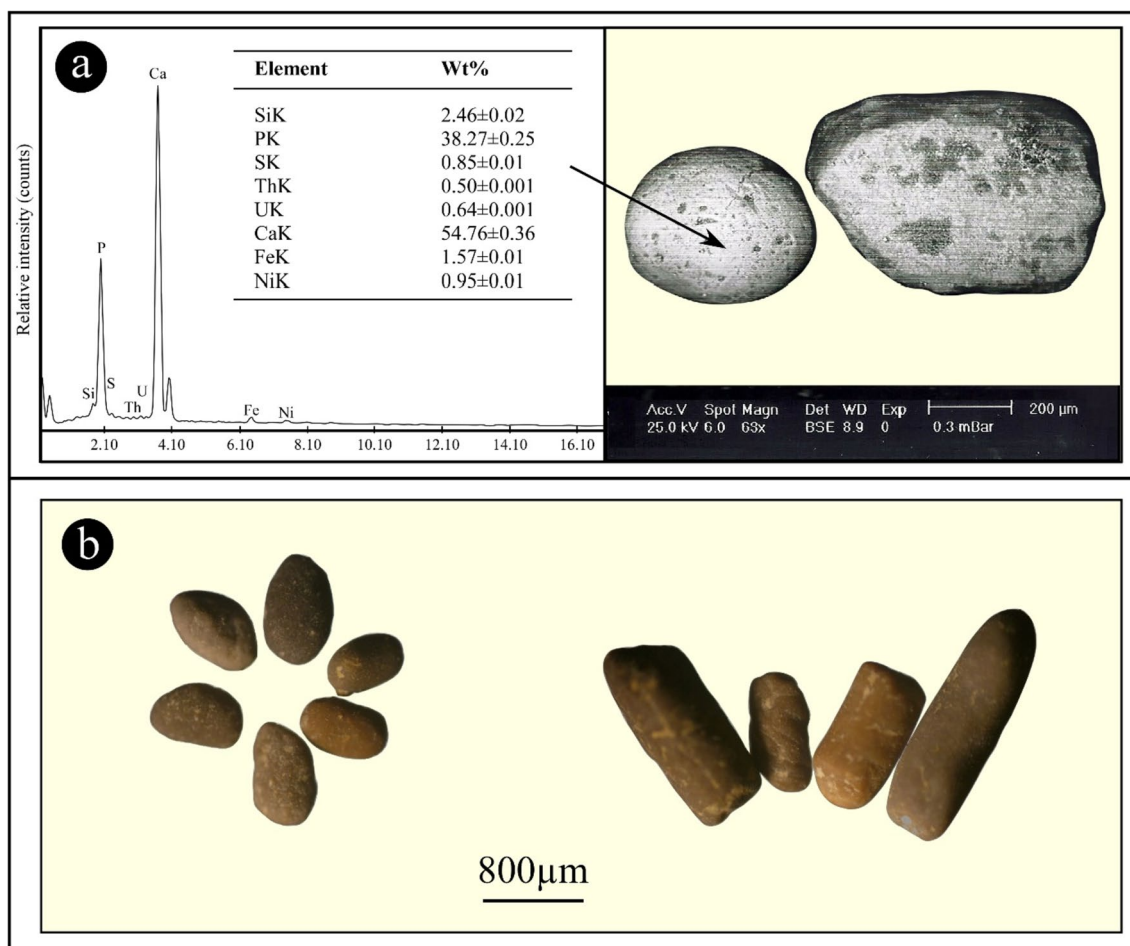


Fig. 6 **a** Energy Dispersive X-ray (EDX) and Back Scattered Electron image (BSE) showing well-rounded peloid of apatitic composition. **b** Stereo photomicrograph showing different varieties of apatite minerals

Fe, Ti, Cr, Ni, Al, and Zn. The presence of a relatively high Si concentration in the bone fragment supports slight displacement with the major component as a probable diagenetic process.

Geochemistry

Twelve representative samples (six samples from each side) were subjected to chemical investigation after well and careful quartering to ensure homogeneity. The resultant data for the major and trace components (Table 2 and 3) point to clear variability between the studied phosphorites on both sides of the Nile Valley.

The east side phosphorites have higher average contents of P_2O_5 , CaO, and F than their corresponding in the west side (Fig. 8). Such a remark is in good alignment with the relative abundance of the phosphatic components as revealed by the mineralogic investigation, while the SiO_2 average on

both sides showed clear enrichment in the west side, which is considered a good reflection of the abundance of quartz grains in the west phosphorites, either as detrital grains or cementing material.

Also, the relative abundance of Fe_2O_3 , organic content (the loss at 550 °C), and approximately all the trace elements are noticed in the eastern phosphorites compared to the western ones. Such abundance of trace elements is likely ascribed to the higher organic content in the eastern phosphorites, where the organic materials play an important role in the adsorption and accumulation of most of these trace elements within the phosphorite deposits [28–30]. The noticed apatite abundance in the East phosphorites, as revealed by the mineralogical investigation, is another probable reason for the relative enrichment of Sr, Ba, and Zn, where these elements have a marked affinity towards fixation in the apatite crystal lattice [31].

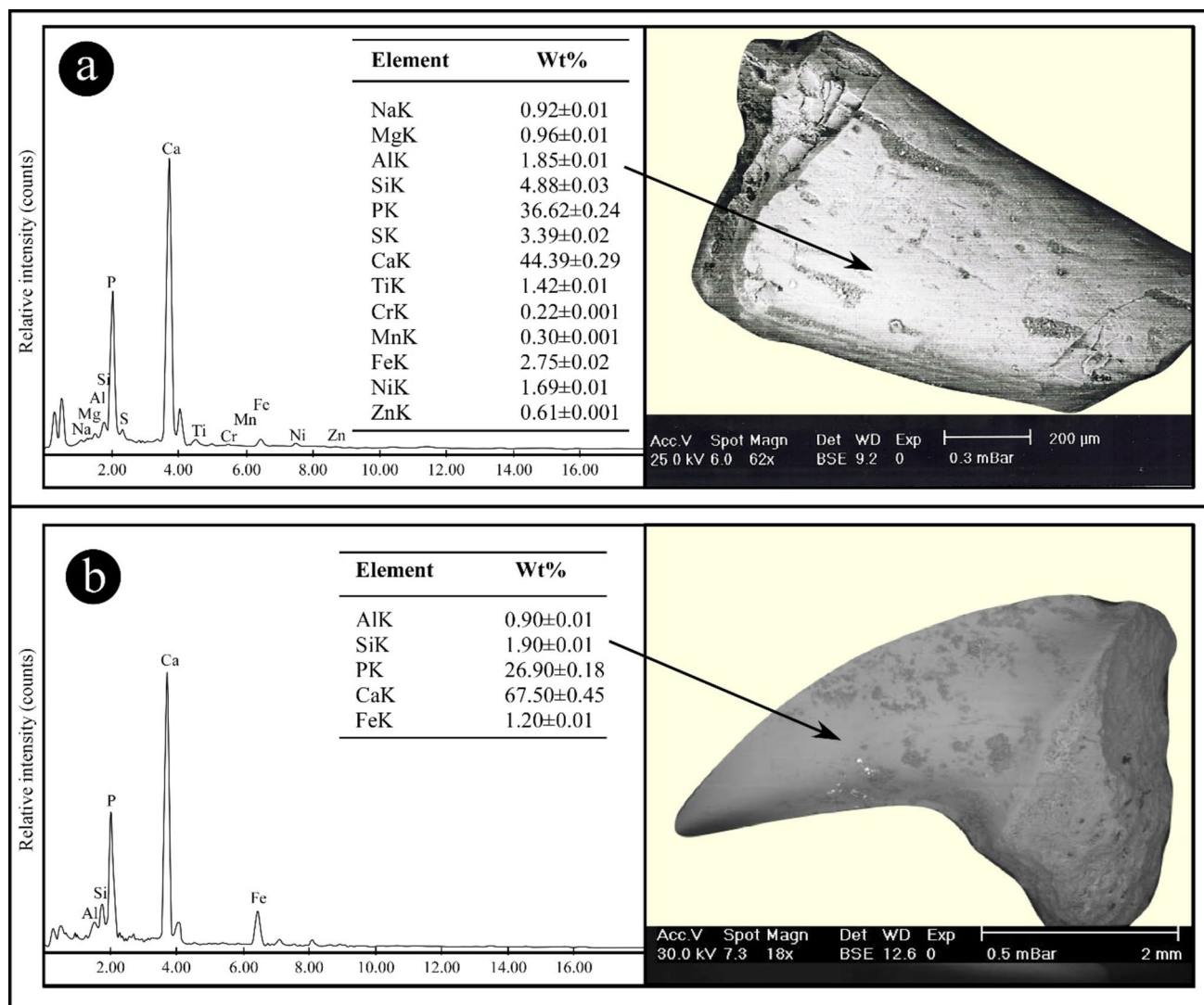


Fig. 7 EDX pattern and BSE photomicrograph showing **a** bone fragment and **b** shark teeth

On the other hand, the Zr element behaves differently compared to the other trace elements, where it exhibits slight enrichment in the western phosphorites. Such observations are accepted in light of the marked abundance of detritals in the western phosphorites, where Zr in some phosphorites exists in detrital phases, substituting for Ti in titaniferous minerals such as ilmenite [32].

The CaO/P₂O₅ ratio in the studied phosphorites is considered a relatively high ratio compared to the normal ratio, which is 1:1.23 [33]. To understand the reason for this elevated ratio, we have to refer to the mineralogical investigation using the XRD, where both calcite (CaCO₃) and gypsum (CaSO₄) minerals were recorded in the studied phosphorites, and for sure, these minerals have a partial contribution to the high CaO content of the whole rock's chemical composition. Additionally, and as will be shown

later, the potential effect of the acidified water on the apatite grains has a reverse effect on the P₂O₅ content, particularly on the western side. Consequently, the P₂O₅/CaO ratio (in average) was increased to 1:1.37 and 1:1.78 in the eastern and western phosphorites, respectively.

A chemical map of the apatite grains from the phosphorites on both Nile Valley sides was carried out using the microprobe technique. The elemental distribution shows the P:Ca ratio as 1.4 and 1.7 in the eastern and western phosphorites, respectively (Figs. 9, 10 and 11), which confirmed the relative abundance of apatite mineral on the eastern side. Also, the same observation was found with the iron distribution, which can be attributed to its abundance in the matrix as cement material.

Table 2 Major oxides concentrations of the studied phosphorite

Samples	Oxides											Loss on ignition			
	P ₂ O ₅	CaO	Fe ₂ O ₃	MgO	SiO ₂	Al ₂ O ₃	Na ₂ O	K ₂ O	TiO ₂	SO ₄ ²⁻	F ⁻	110 °C	550 °C	1000 °C	
E-1	24.15±0.16	38.11±0.25	3.79±0.03	3.84±0.03	10.36±0.07	5.10±0.03	1.37±0.01	0.26±0.002	0.01±0.001	0.23±0.002	2.31±0.02	0.18±0.001	2.58±0.02	5.62±0.04	
E-2	28.11±0.19	39.02±0.26	3.8±0.03	2.89±0.02	8.12±0.05	4.32±0.03	1.45±0.01	0.30±0.002	0.01±0.001	0.15±0.001	2.66±0.02	0.29±0.002	2.86±0.02	4.12±0.03	
E-3	31.16±0.21	42.86±0.28	3.99±0.03	3.27±0.02	6.66±0.04	1.58±0.01	1.34±0.01	0.28±0.002	0.02±0.001	0.18±0.001	2.27±0.01	0.59±0.004	2.89±0.02	3.45±0.02	
E-4	32.01±0.21	41.87±0.28	4.09±0.03	2.75±0.02	7.01±0.05	1.65±0.01	1.11±0.01	0.31±0.002	0.02±0.001	0.33±0.002	3.12±0.02	0.43±0.003	3.03±0.02	3.23±0.02	
E-5	30.72±0.20	41.2±0.27	4.01±0.03	2.42±0.02	7.8±0.05	2.56±0.02	1.18±0.01	0.19±0.001	0.01±0.001	0.21±0.001	2.20±0.01	0.75±0.005	2.97±0.02	3.64±0.02	
E-6	31.05±0.20	40.34±0.27	4.23±0.03	1.99±0.01	8.01±0.05	2.17±0.01	0.99±0.01	0.22±0.001	0.01±0.001	0.26±0.002	2.76±0.02	0.58±0.004	3.11±0.02	3.48±0.02	
Aver- age ± S. E	29.53±1.20	40.57±0.72	3.99±0.069	2.86±0.07	7.99±0.52	2.90±0.60	1.24±0.07	0.26±0.02	0.013±0.002	0.23±0.025	2.55±0.14	0.47±0.08	2.91±0.07	3.92±0.36	
W-1	21.74±0.14	37.4±0.25	2.79±0.02	2.42±0.02	23.72±0.16	0.65±0.00	0.69±0.01	0.09±0.001	0.06±0.001	0.10±0.001	1.95±0.01	1.09±0.007	2.11±0.01	6.2±0.04	
W-2	21.23±0.14	38.13±0.25	1.99±0.01	3.01±0.02	21.86±0.14	0.77±0.01	0.81±0.01	0.12±0.001	0.07±0.001	0.12±0.001	2.10±0.01	0.89±0.006	1.66±0.01	5.49±0.04	
W-3	22.61±0.15	40.10±0.26	2.4±0.02	3.63±0.02	18.60±0.12	1.37±0.01	0.69±0.01	0.14±0.001	0.06±0.001	0.09±0.001	2.05±0.01	0.99±0.007	2.32±0.02	3.83±0.03	
W-4	21.89±0.14	39.78±0.26	2.14±0.01	3.55±0.02	20.1±0.13	1.19±0.01	0.66±0.01	0.09±0.001	0.05±0.001	0.11±0.001	1.88±0.01	1.10±0.007	1.85±0.01	4.11±0.03	
W-5	19.18±0.13	31.90±0.21	4.19±0.03	3.80±0.3	25.63±0.17	2.10±0.01	0.90±0.01	0.10±0.001	0.31±0.002	0.12±0.001	1.95±0.01	0.87±0.006	1.75±0.01	6.38±0.04	
W-6	20.14±0.13	38.37±0.25	3.26±0.02	2.99±0.02	23.27±0.15	1.88±0.01	0.84±0.01	0.09±0.001	0.26±0.002	0.08±0.001	1.79±0.1	0.91±0.006	1.39±0.01	5.18±0.03	
Aver- age ± S. E	21.09±0.51	37.61±1.21	2.79±0.33	3.23±0.21	22.19±1.01	1.33±0.23	0.77±0.04	0.11±0.008	0.14±0.047	0.10±0.006	1.95±0.04	0.81±0.04	1.85±0.13	5.20±0.42	

Radioactivity

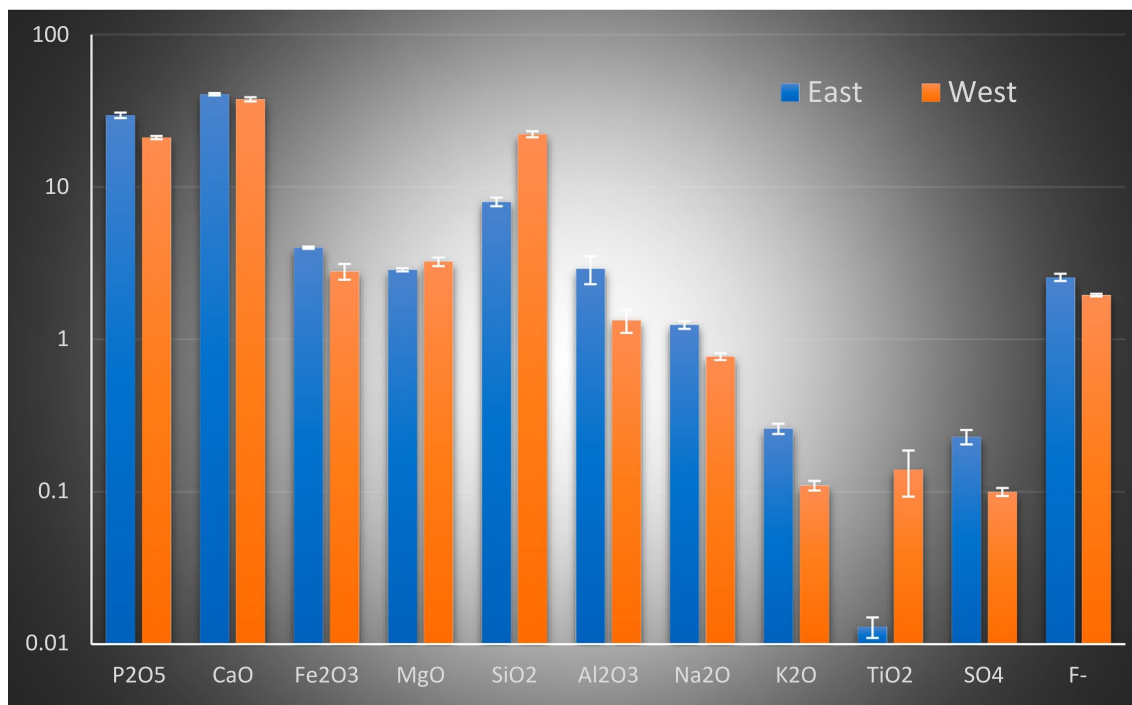
The radioelement contents were determined as equivalent uranium (eU), equivalent thorium (eTh), and Ra in both East and West Nile Valley phosphorites using the NaI-gamma spectrometer (Table 4). The obtained data clearly point out that the eastern phosphorites have higher radioelement concentrations (averages of eU, eTh, and Ra equal 91.7, 5.33, and 96.83 ppm, respectively) than the western phosphorites (averages of eU, eTh, and Ra equal 44.83, 2 and 55.33 ppm, respectively). It was expected that the uranium and its subsequent daughter Ra are approximately equal on both the phosphorites where they were deposited in the same basin under the same environment and geochronological conditions, but this is not the current situation. This observation strongly supports the occurrence of diagenetic processes that affect the original uranium contents of the studied phosphorites, causing either uranium enrichment in the eastern phosphorites or uranium depletion in the western ones. The P-factor can give us a good idea of which process happened and affected the uranium concentrations.

The P-factor is the output value of eU/Ra [34, 35] and is used as an indicator for the uranium enrichment or depletion, where the P-factor equal to one means no diagenetic processes affect the uranium content after its deposition (i.e., the uranium content is in equilibrium with its Ra daughter since its formation), while the value greater than one suggests uranium enrichment and the value less than one means uranium removal or depletion (i.e., the case of the uranium disequilibrium). Referring to the calculated P-factor of the studied phosphorite samples (Table 4), it is easily concluded that both phosphorites were subjected to uranium removal, but such removal was faint in the eastern phosphorites (P-factor equals 0.94 on average), while the uranium removal in the western phosphorites was deeper (P-factor equals 0.8 on average). Uranium, in its hexa-valance status, is known for its ability to mobilize under the conditions of weathering, alteration, and/or the presence of a removal and leaching agent [34, 36–39]. The easiest mobilized uranium, which is adsorbed onto the surfaces of some components such as; mica flakes, iron oxides, organic matter, and uranium encountered in the mineral crystal structure, could be mobilized to a lesser extent under the availability of some conditions, like mineral metamictization and/or attack by an acidified dissolution agent [40–45].

Accordingly, referring to the chemical analysis of the studied phosphorites, we can draw a reasonable conclusion about the uranium variance between these phosphorites through the binary relation and correlation coefficient of eU with P₂O₅, Fe₂O₃, and the organic content (obtained by ignition at 550 °C) (Fig. 12).

Table 3 Trace elements concentrations of the studied phosphorites

Samples	Elements									
	Cr	Ni	Cu	Zn	Zr	Rb	Y	Ba	Sr	V
E-1	125±0.83	18±0.12	14±0.09	135±0.89	10±0.07	33±0.22	84±0.55	796±5.3	1167±7.7	147±0.97
E-2	124±0.82	16±0.11	13±0.09	137±0.90	11±0.07	29±0.19	80±0.53	790±5.2	1211±8.0	150±0.99
E-3	125±0.83	12±0.08	14±0.09	142±0.94	11±0.07	25±0.17	40±0.26	769±5.1	1812±12.0	170±1.12
E-4	126±0.83	17±0.11	15±0.10	139±0.92	12±0.08	34±0.22	66±0.44	750±5.0	1190±7.9	155±1.02
E-5	123±0.81	14±0.09	13±0.09	150±0.99	10±0.07	29±0.19	59±0.39	742±5.0	1717±11.3	167±1.10
E-6	120±0.79	13±0.09	12±0.08	135±0.89	12±0.08	28±0.18	79±0.52	710±4.7	1350±8.9	156±1.03
Average ± S.E	124±0.87	15±0.96	14±0.42	140±2.33	11±0.36	30±1.35	68±6.8	760±13.10	1408±116.40	158±3.74
W-1	108±0.71	11±0.07	13±0.09	120±0.79	17±0.11	28±0.18	93±0.61	566±3.7	1126±7.4	63±0.42
W-2	112±0.74	12±0.08	11±0.07	125±0.83	15±0.10	27±0.18	86±0.57	610±4.0	1150±7.6	75±0.50
W-3	140±0.92	16±0.11	12±0.08	120±0.79	19±0.13	25±0.17	81±0.53	808±5.0	1273±8.4	106±0.70
W-4	138±0.91	14±0.09	12±0.08	119±0.79	16±0.11	22±0.15	84±0.55	790±5.2	1090±7.2	93±0.61
W-5	98±0.65	18±0.12	13±0.09	120±0.79	16±0.11	32±0.21	80±0.53	600±4.0	961±6.3	55±0.36
W-6	106±0.70	16±0.11	10±0.07	115±0.76	13±0.09	26±0.17	79±0.52	620±4.1	1016±6.7	86±0.57
Average ± S.E	117±7.20	15±1.01	12±4.77	120±1.30	16±0.81	27±1.35	84±2.12	666±42.87	1103±44.54	80±7.78

**Fig. 8** A histogram shows the averages of the major chemical components in both the East and West Nile Valley phosphorites

The eU-P₂O₅ binary relation in the investigated samples of eastern and western phosphorites resulted in a strong correlation (0.94 and 0.75, respectively); these correlation values indicate the presence of syngenetic uranium. They also point out that the apatite mineral in the western phosphorites was affected to some extent by the diagenetic

removal process, which caused a low-P₂O₅% compared to its percentage in the eastern phosphorites as well as the removal of some uranium content. In contrast, the eU-Fe₂O₃ and eU-organic content binary relations showed a significant difference between both sides, where a strong correlation is available on the eastern side and a weak or

Fig. 9 Beam scanner dot photograph showing phosphorus distribution in apatite grain and the matrix in the studied samples (**a** East side and **b** West side)

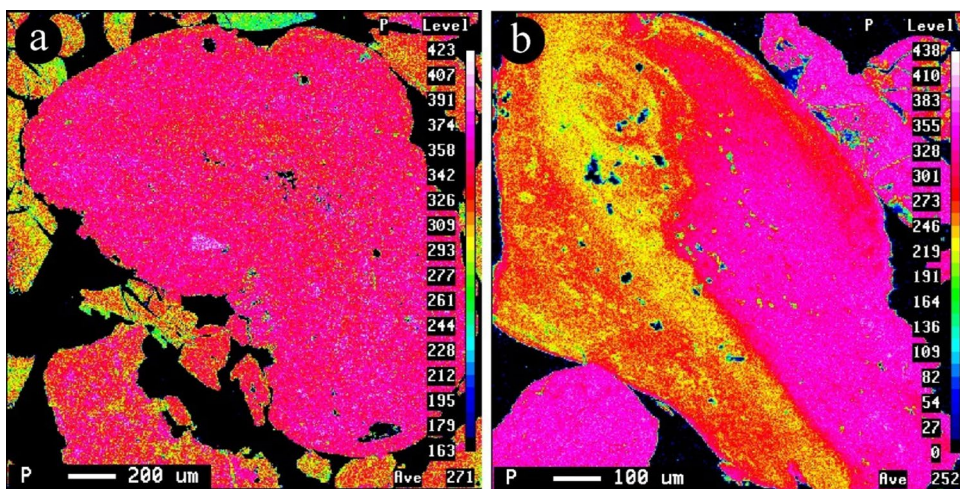


Fig. 10 Beam scanner dot photograph showing calcium distribution in apatite grain and the matrix in the studied samples (**a** East side and **b** West side)

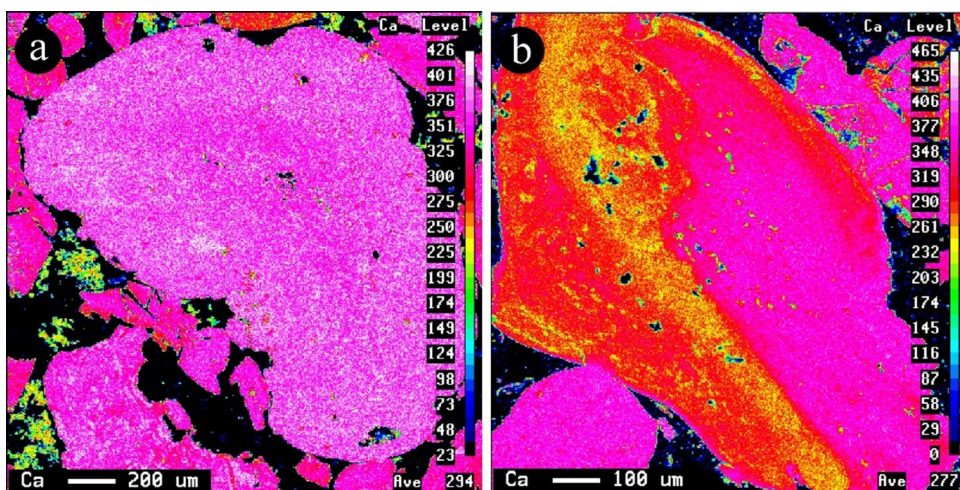


Fig. 11 Beam scanner dot photograph showing iron distribution in apatite grain and the matrix in the studied samples (**a** East side and **b** West side)

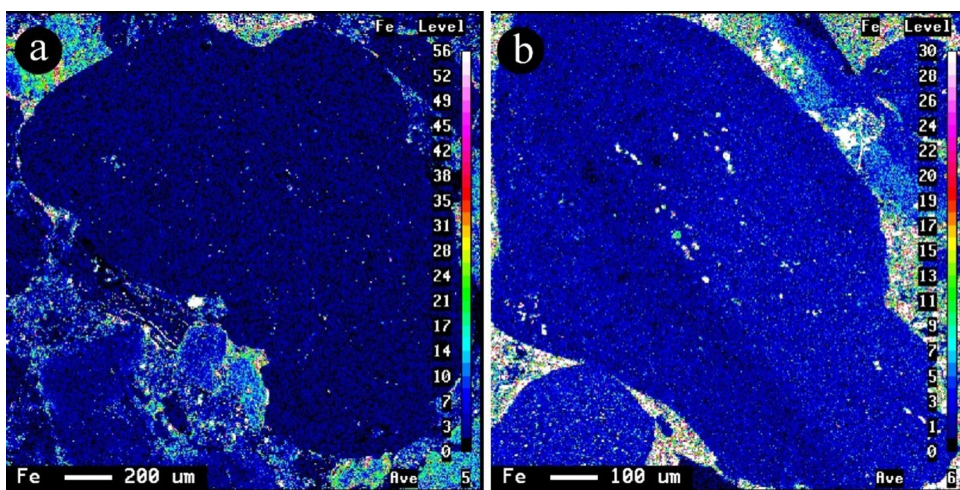


Table 4 Equivalent uranium contents (eU), equivalent thorium contents (eTh) and radium contents (Ra) of the studied phosphorites

Sample no.	eU (ppm)	eTh (ppm)	Ra (ppm)	P-factor (eU/Ra)
E-1	74	4	82	0.90
E-2	79	5	85	0.93
E-3	97	7	105	0.92
E-4	100	7	103	0.97
E-5	98	3	101	0.97
E-6	102	6	105	0.97
Average ± S.E	91.7 ± 4.9	5.33 ± 0.6	96.83 ± 4.27	0.94 ± 0.013
W-1	59	1	67	0.88
W-2	52	2	64	0.81
W-3	45	3	52	0.87
W-4	48	3	59	0.81
W-5	30	2	40	0.75
W-6	35	1	50	0.70
Average ± S.E	44.83 ± 4.39	2 ± 0.36	55.33 ± 4.10	0.80 ± 0.029

no correlation on the western side. Such remarks strongly suggest a wide removal of the diagenetic uranium that adsorbed onto the iron mineralogical and organic components of the western phosphorites.

Also, the higher SO_4^{2-} concentration (Table 4) in the eastern bank (0.23% in average) than the western one (0.08% in average) might indicate dissolution of some sulfide components in the western phosphorites under the effect of the ground water, which increases the removal of the adsorbed uranium due to the slight acidification of the dissolution agent. This assumption takes us to determine the reason that made the apatite mineral amount and the P_2O_5 content in the western phosphorites lower than in the eastern one, where the slightly acidified water has the capability to dissolve part of the present apatite, and hence some of the P_2O_5 content.

Finally, in light of this result about the role played by groundwater, a logic reason is needed to interpret the wide availability of groundwater on the western side. This phenomenon could be attributed to the nature of the basement rocks on which the phosphorites were deposited during the marine transgression episode, where the eastern side is nearer to the high elevated basement rocks mountains in the Eastern Desert, Egypt, which might cause a relative elevation in the eastern side than the western part, and hence led to a relative land tilting toward the west, which enforced the groundwater migration in the same direction.

Conclusions

The Nile valley phosphorite deposits on both the eastern and western sides showed a significant difference in the main chemical components, where the P_2O_5 values recorded 29.53 and 21.09%, while the CaO values were 40.57 and 37.61% in the eastern and western phosphorites, respectively. Moreover, the uranium content in the eastern phosphorites has more than twice the value in the eastern phosphorites (91.7 ppm on average) as its value in the western phosphorites (44.83 ppm on average). The calculated P-factor (eU/Ra) as an indicator for uranium enrichment (> 1) or uranium depletion (< 1) pointed to a significant uranium depletion in the western phosphorites (P-factor equals 0.8) and a very faint depletion in the eastern one (P-factor equals 0.97). On the other hand, the strong correlation in the binary relation of eU- Fe_2O_3 and eU-organic content (0.92 and 0.89, respectively) for the eastern phosphorites strongly supports the presence of respectful diagenetic uranium due to adsorption of the uranium hexa-valence (U^{6+}) onto surfaces of the iron oxide and organic components, while the similar correlation values (-0.75 and 0.47) in the western phosphorites point to considerable removal of the diagenetic uranium (U^{6+}), which is easily mobile under the effect of removal agents like the acidified water. This conclusion well matches the calculated p-factors as shown above. Finally, a collective conclusion about the reason for the uranium variance between the eastern and western sides of the Nile Valley phosphorites could be figured as follows: a considerable amount of the uranium content in the Nile Valley phosphorites was diagenetically formed through its adsorption onto the iron oxides and organic components as hexavalent uranium. The groundwater played a key role in the removal of considerable uranium content, causing the detected variance in the uranium concentration between both sides. Sulfide minerals contributed to the groundwater forming slightly acidified water, which caused the relative dissolution of the encountered uranium, particularly from the western phosphorites, as well as some phosphorous components.

Funding Open access funding provided by The Science, Technology & Innovation Funding Authority (STDF) in cooperation with The Egyptian Knowledge Bank (EKB).

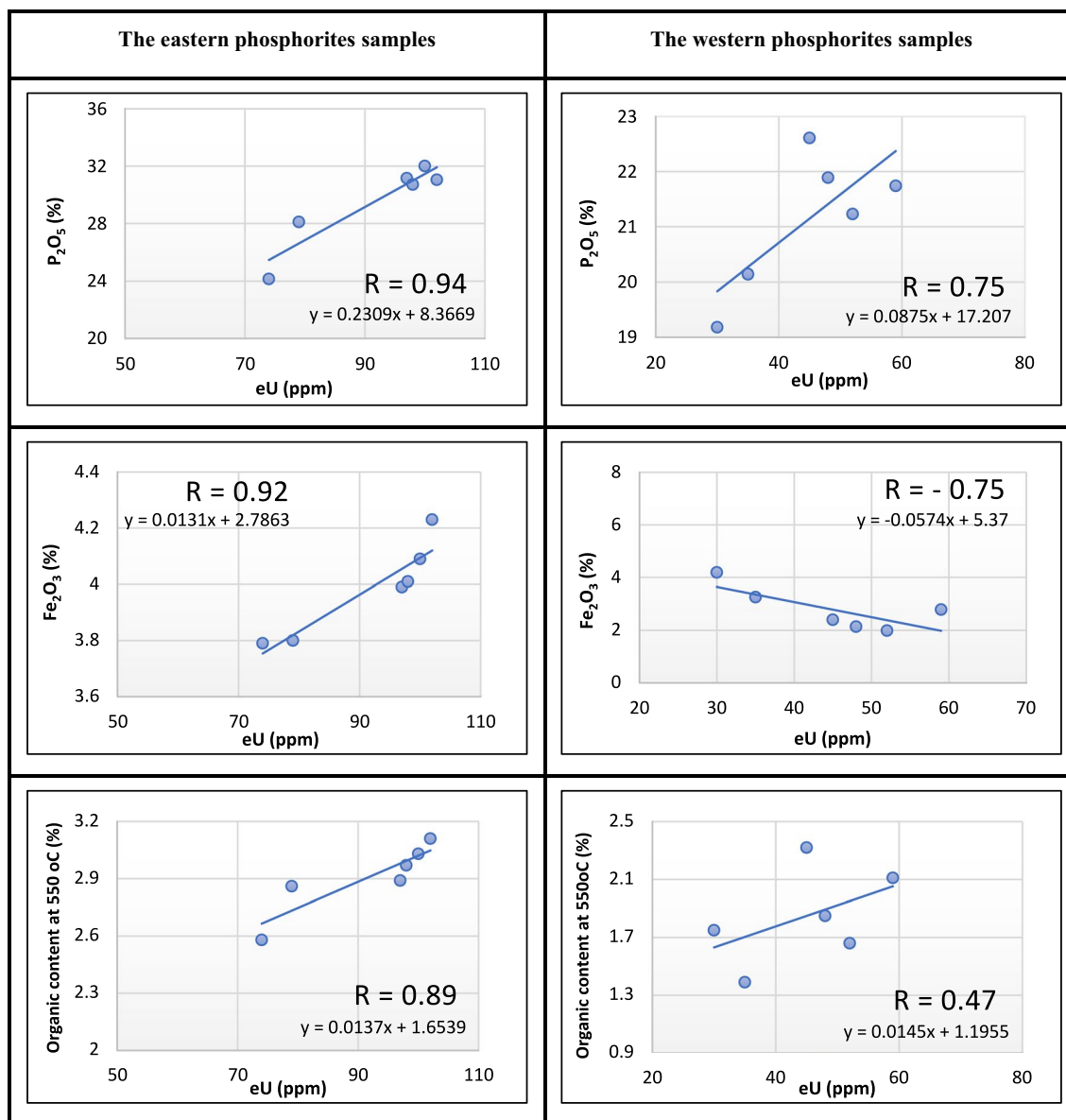


Fig. 12 The binary relation and correlation coefficient values of eU with P_2O_5 , Fe_2O_3 and the organic matter contents

Declarations

Conflict of interest The author declares that he has no known competing financial interests or personal relationships that could have appeared to influence the work reported in this paper.

Open Access This article is licensed under a Creative Commons Attribution 4.0 International License, which permits use, sharing, adaptation, distribution and reproduction in any medium or format, as long as you give appropriate credit to the original author(s) and the source, provide a link to the Creative Commons licence, and indicate if changes were made. The images or other third party material in this article are

included in the article's Creative Commons licence, unless indicated otherwise in a credit line to the material. If material is not included in the article's Creative Commons licence and your intended use is not permitted by statutory regulation or exceeds the permitted use, you will need to obtain permission directly from the copyright holder. To view a copy of this licence, visit <http://creativecommons.org/licenses/by/4.0/>.

References

- Cook PJ, Shergold JH (2005) Phosphate deposits of the world: volume 1: Proterozoic and Cambrian phosphorites. Cambridge University Press, USA
- Elmaadawy KG, Ezz El Din M, Khalid A, Abouzeid A (2015) Mineral industry in Egypt—part II non metallic commodities—phosphate rocks. *J Min World Express* 4:1–18
- El Bamiki R, Raji O, Ouabid M, Elghali A, Khadiri Yazami O, Bodinier J-L (2021) Phosphate rocks: a review of sedimentary and igneous occurrences in Morocco. *Minerals* 11:1137
- Van Kauwenbergh SJ (2010) World phosphate rock reserves and resources. *Ifdc Muscle Shoals*
- Chen M, Graedel TE (2015) The potential for mining trace elements from phosphate rock. *J Clean Prod* 91:337–346. <https://doi.org/10.1016/j.jclepro.2014.12.042>
- Khalil M, Denchi M (2002) Basins geometry and tectonic origin of the western Desert of Egypt, relevance to economic resources. In: *Proceedings of the 5th international conference on the geology of the Arab World*, Cairo University II, 2000, pp 523–542
- Germann K, Bock W-D, Schröter T (1985) Properties and origin of Upper Campanian phosphorites in Egypt. *Sci Géol Bull Mém* 77:23–33
- Baioumy H, Tada R (2005) Origin of late Cretaceous phosphorites in Egypt. *Cretac Res* 26:261–275
- Baioumy H, Tada R, Gharaie M (2007) Geochemistry of Late Cretaceous phosphorites in Egypt: implication for their genesis and diagenesis. *J Afr Earth Sci* 49:12–28
- Bishady AM, Farag NM, Mira HI, Elsayey E-SH, Negm SH (2019) a contribution to the geochemistry of El-Sibaiya phosphorites, Nile Valley, Egypt. *Nucl Sci Sci J* 8:39–58
- El-Kammar A (1970) Mineralogical and geochemical studies on El-Hagarin El-Mossattaha phosphate, Sibaiya East. Cairo University Egypt
- Mansour AM, Osman MR, Khaleal FM, Elshazly MM (2023) Geology and geochemistry of the phosphorite deposits, Sibaiya Area, Nile Valley, Egypt. *Arab J Nucl Sci Appl* 56:53–74
- Negm SH (2014) Radioactivity and geochemical studies of the Nile Valley phosphorites. Minufiya University, Egypt
- Gaafar I, Hanfi M, El-Ahli LS, Zeidan I (2021) Assessment of radiation hazards from phosphate rocks, Sibaiya area, central eastern desert, Egypt. *Appl Radiat Isotopes* 173:109734
- Mansour MG, El-Moghny MWA, Zidan IH, Hassaan MM (2023) Characterization, and potential of subsurface phosphorite bearing uranium at East Mahameid Region, Egypt. *Al Azhar Bull Sci* 34:5
- Cook PJ (1972) Petrology and geochemistry of the phosphate deposits of Northwest Queensland, Australia. *Econ Geol* 67:1193–1213
- El-Kammar A, El-Kammar M (2002) On the trace elements composition of the Egyptian phosphorites: a new approach. In: *Sixth international conference on geology of the Arab World*, Cairo Univ, 2002, pp 227–244
- El-Arabi AE-GM, Khalifa IH (2002) Application of multivariate statistical analyses in the interpretation of geochemical behaviour of uranium in phosphatic rocks in the Red Sea, Nile Valley and Western Desert, Egypt. *J Environ Radioact* 61:169–190
- Salman A (1974) Structure and radioactivity of some phosphate deposits, East Luxor Area, Eastern Desert, Egypt. Ph. D. thesis, Fac. of Sci. Ain Shams Univ
- Abdou N (2002) Distribution of uranium, thorium and rare earth elements in some Egyptian phosphorites. In: *Proceed 13th symp Phaner Develop*, Egypt, pp 213–224
- Gindy AR (1978) Alpha radioactivity of the constituent particles in some pelletal phosphorites from Safaga and other localities in Egypt. *J Sediment Res* 48:539–544
- Said R (2017) *The geology of Egypt*. Routledge
- Glenn CR, Arthur MA (1990) Anatomy and origin of a Cretaceous phosphorite-greensand giant, Egypt. *Sedimentology* 37:123–154
- Ghanem M, Zalata A, El-Razek TMA, Mikhailov IA, Rasvaliev AV, Mirtov YV (1968) Report on the results of prospecting and geological surveying for phosphorites in the area between the towns of Idfu and Qena, Nile Valley. Geological Survey of Egypt, (EGSMA)
- Philobos ER (1969) Geology of the phosphoate of the Nile Valley, Egypt. Assuit University
- Shapiro L, Brannock WW (1962) Rapid analysis of silicate, carbonate and phosphate rocks, vol 1144. US Government Printing Office
- El-Reedy M (1984) The general physical and chemical features and the pollution level of El-Sabahia–SabhanSabhan–El Reqa soil localities, state of Kuwait Internal Report Environmental Protection Dept., Ministry of Pub. Health–El Kuwait (Part 1: chemical methods)
- Tooms J (1969) Geochemistry of marine phosphate and manganese deposits. *Oceanogr Mar Biol Ann Rev* 7:49–100
- Mohamed MS (1979) Geochemical and petrological investigation on the phosphatic rocks of Sharawna-Mahamid district, Nile Valley. Assiut University
- Soliman M, Ahmed E, Kurzweil H (2006) Geochemistry and mineralogy of the Paleocene/Eocene boundary at Gabal Dababiya (GSSP) and Gabal Owaina sections, Nile Valley, Egypt. *Stratigraphy* 3:31–53
- Altschuler Z (1980) The geochemistry of trace elements in marine phosphorites: part I. Characteristic abundances and enrichment
- Pacey N (1984) Electron paramagnetic resonance spectrometry of samples from the English chalk. An integrated study. *Med Geol* 8:241–248
- Gilmour R (2013) Phosphoric acid: purification, uses, technology, and economics. CRC Press
- El Galy M (2007) Mobilization of some radioelements and its implication on their favorability, case study on selected granitic plutons, Central Eastern Desert, Egypt. *Sci J Fac Sci* 21:19–38
- Hussein A (1978) Lecture course in nuclear geology. Ain Shams University (unpublished)
- Stuckless J, Nkomo I, Wenner D, Vantrump G (1984) Geochemistry and uranium favourability of the postorogenic granites of the Northwestern, Arabian shield, Kingdom of Saudi Arabia
- China National Nuclear Corporation C (1993) Research achievement from Bureau of Geology
- Yan X, Luo X (2015) Radionuclides distribution, properties, and microbial diversity of soils in uranium mill tailings from south-eastern China. *J Environ Radioact* 139:85–90. <https://doi.org/10.1016/j.jenvrad.2014.09.019>
- Payne TE (1991) A study of uranium and thorium migration at the Koongarra uranium deposit with application to actinide transport from nuclear waste repositories
- Wang Z, Lee S-W, Catalano JG, Lezama-Pacheco JS, Bargar JR, Tebo BM, Giammar DE (2013) Adsorption of uranium (VI) to manganese oxides: X-ray absorption spectroscopy and surface complexation modeling. *Environ Sci Technol* 47:850–858
- Zhang X, Zhang L, Liu Y, Li M, Wu X, Jiang T, Chen C, Peng Y (2020) Mn-substituted goethite for uranium immobilization:

- a study of adsorption behavior and mechanisms. *Environ Pollut* 262:114184
42. Barnett M, Jardine P, Brooks S, Selim H (2000) Adsorption and transport of uranium(VI) in subsurface media. *Soil Sci Soc Am J*. <https://doi.org/10.2136/sssaj2000.643908x>
 43. Sanpawanitchakit C (2003) The application of surface complexation modeling to the adsorption of uranium (VI) on natural composite materials
 44. Lenhart JJ (1997) Application of surface complexation modeling to the adsorption of uranium (VI) onto hematite in the presence of humic and fulvic acids. The 1990–1999-Mines Theses & Dissertations
 45. McGloin M, Tomkins A, Webb G, Spiers K, MacRae C, Paterson D, Ryan C (2015) Release of uranium from highly radiogenic zircon through metamictization: the source of orogenic uranium ores. *Geology* 44:15–18. <https://doi.org/10.1130/G37238.1>

Publisher's Note Springer Nature remains neutral with regard to jurisdictional claims in published maps and institutional affiliations.